International Journal of Applied Engineering Research ISSN 0973-4562 Volume 13, Number 7 (2018) pp. 5008-5013

Preparation and Characterizations of Poly (vinylidene fluoride) (PVDF)/$Ba_{0.6}Sr_{0.4}TiO_3$ (BST) Nanocomposites

Sabah A. Salman*, Farah T. M. Noori, Aws K. Mohammed***

**University of Diyala, College of Science, Physics Dept., Diyala, Iraq.*

*** University of Baghdad, College of Science, Physics Dept., Baghdad, Iraq.*

Abstract

Poly(vinylidene fluoride) (PVDF) / Barium Strontium Titanate (BST) nanocomposites with BST filler contents of 0–20 vol% have been fabricated by using solution casting method. The structural and dielectric properties of PVDF/BST nanocomposites have been investigated. The structural properties of PVDF/BST nanocomposites have been studied using X-ray diffraction. The XRD results showed that the BST nanopowder obtained by hydrothermal method with a perovskite structure and the α and γ- PVDF crystalline phases appeared at pure PVDF and nanocomposites samples. The crystallite size was calculated using Scherrer and Williamson-Hall (W-H) equations and it is observed that the crystallite size increase as the content of BST filler increases from 5 to 20 vol%. The frequency dependency of dielectric constant, dielectric losses and AC conductivity of the PVDF/BST naocomposites with different volume fractions of BST filler in frequency range 50Hz–1MHz at room temperature were studied. The dielectric constant of the PVDF/BST nanocomposites increases from 17.5 to 26.3 (at 100 kHz) with BST filler increasing from 0 vol% (pure PVDF) to 20 vol%. The dielectric losses and AC conductivity of the PVDF/BST nanocomposites increase with BST filler increasing at the same frequency. The dielectric properties of PVDF were improved by increasing BST filler.

Keywords: PVDF/BST nanocomposites, Structural Properties, Dielectric Properties.

INTRODUCTION

In the recent years, material scientists are putting lots of interest for the development of new multifunctional ceramic, polymer, polymer composite materials for many device applications in electronics and optoelectronic industry. In view of the above, polymer-ceramic composites have received a significant attention in view of their technological importance in devices such as high energy density capacitors, sensors, actuators, transducers etc. The fabrication of composites is to combine two or more different materials/phases having different properties to obtain the suitable material properties that often cannot be obtained in single-phase materials. In the context of energy storage device, ferroelectric ceramic polymer composites have been studied world-wide [1-3]. In the last decades, high dielectric constant ferroelectric ceramics such as $Pb(Zr,Ti)O_3$ (PZT) and $BaTiO_3$ (BT) have been used as fillers in polymer based composites with high dielectric constant and dielectric breakdown strength. The ceramic fillers used to achieve polymer based composites with high dielectric constant and dielectric breakdown strength are limited to ferroelectric ones [4–6]. Ferroelectric Barium Strontium Titanate (BST) has acquired much attention due to their large dielectric constant, composition dependent Curie temperature, high tunable and ferroelectric properties. It is an interesting material for applications such as multilayer ceramic capacitors [7], piezoelectric and pyroelectric sensors. Hydrothermal synthesis is attractive because it is environmentally benign, a one-step process, low temperature (<200°C), and uses inexpensive starting materials.

Polyvinylidene fluoride (PVDF) is a semi-crystalline polymer having remarkable thermal stability, good chemical resistance and extraordinary pyroelectric and piezoelectric properties among polymers. These properties combined with its high elasticity, relative transparency and ease of processing, make this material suitable for various technological applications [2,8]. PVDF shows a complex structure and it can exhibit five distinct crystalline phases related to different chain conformations, known as α, β, γ, δ and ε phases. Thus, the use of PVDF as matrix in nanocomposites is one of the key parameters for a wide range of applications. The final properties of these nanocomposites mainly depend on parameters such as filler content, method of preparation and the dispersion of nanoparticles into the polymer matrix [9–11].

In this work, structural and dielectric properties of Poly(vinylidene fluoride) (PVDF)/$Ba_{0.6}Sr_{0.4}TiO_3$ (BST) nanocomposites were studied. The BST nanopowders were synthesized by hydrothermal method. BST /PVDF nanocomposites were fabricated by using a solution casting method. The effect of content of the BST on the microstructure, and dielectric properties of the nanocomposites were investigated.

EXPERIMENTAL PROCEDURES

The $Ba_{0.6}Sr_{0.4}TiO_3$ (BST) nanopowder were synthesized by hydrothermal method by using Barium Hydroxide ($Ba(OH)_2.8H_2O$) (HiMedia Lab., India), Strontium Hydroxide ($Sr(OH)_2.8H_2O$) (E. Merck, Germany) and Titanium Dioxide (TiO_2) (Central Drug House (P) Ltd., India) as raw materials. The raw materials were mixed with NaOH-KOH mixture and stirred for 1 h by using magnetic stirrer. The final suspension

was transferred to a Teflon vessel of an autoclave, then placed in a digital temperature controlled oven at 160 °C for 12 h. The obtained powder were washed 5 times using distilled water at room temperature and then dried the washed powder in the oven at 80 °C for 10 h. The final product was $Ba_{0.6}Sr_{0.4}TiO_3$ (BST) nanopowder.

The BST nanoparticles were dispersed in an aqueous solution of H_2O_2 (35%) in a magnetic stirrer at 80°C for 2 h, then the powder were washed with distilled water and ethanol and then dried in the oven at 80°C for 6 h.

The Poly(vinylidene fluoride) (PVDF) (3F Co., China) and BST nanopowder were mixed in Dimethylformamide (DMF) solvent with various volume fraction ratio. The mixtures were stirred for 9 h to form stable suspensions. The composite solution was casted on the glass substrate. The film was kept in oven overnight at 50° C to evaporate the DMF solvent. Finally, the PVDF/BST samples were peeled off from the glass substrate. Thickness of the samples was in the range 0.2–0.5 mm measured by digital micrometer.

The X-ray diffraction (XRD-6000, SHIMADZU) are used to study the phase composition of the samples and to calculate crystallite size by using Scherrer and Williamson-Hall equations. Fourier-transform infrared spectroscopy (FTIR) was recorded by using a IRAffinity-1 spectrometer (SHIMADZU). In addition, the dielectric properties were measured using LCR-8105G (GW Instek).

RESULTS AND DISCUSSION

Figure 1 shows FTIR spectra of BST and BST-OH (after reacting with H_2O_2). The band at 550 cm^{-1} is associated to the bond vibration of Ti-O [12]. The bands in the region of 1400 cm^{-1}were attributed to the formation of Ba-O-Ti bond [13]. The new band at 3450 cm^{-1} of BST-OH corresponded to the stretching mode of -OH [12], confirming the surface hydroxylation of the BST. When the BST particles are mixed with PVDF polymer, hydrogen bond will form between the F atoms of PVDF molecular chains and the -OH groups on the surface of the BST particles.

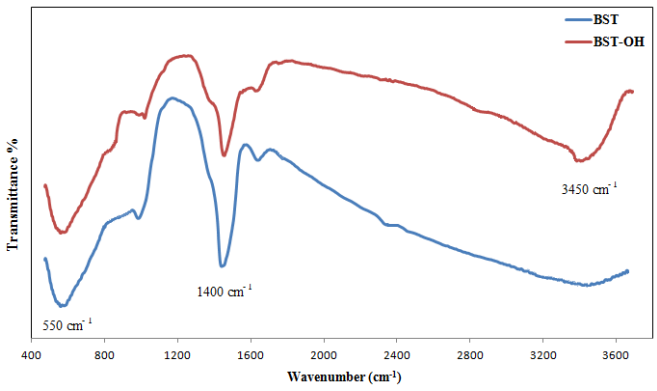

Figure 1. FTIR spectra of the BST and the BST–OH.

The XRD pattern of the BST nanopowder obtained by hydrothermal method is presented in Figure 2. It was shown that the peaks at 2θ that corresponded to 22.4° (100), 31.8° (110), 39.3° (111), 45.69° (200), 51.3° (210) and 56.7° (211) were assigned to BST with a perovskite structure (JCPDS Card No. 34-0411). The intensity of the (110) peak is significantly larger compared to other the peaks. No secondary phases were observed. In Figure 3 one obvious strong peak at 2θ = 20° and three weak peaks at 2θ =18.3°, 26.1° and 38.7° were observed. The peaks at 2θ= 20° and 38.7° were related to (110) and (211) crystalline peaks of γ-PVDF crystalline phase, and the peaks at 2θ=18.3° and 26.1° were related to (020) and (021) crystalline peaks of α- PVDF phase [14].

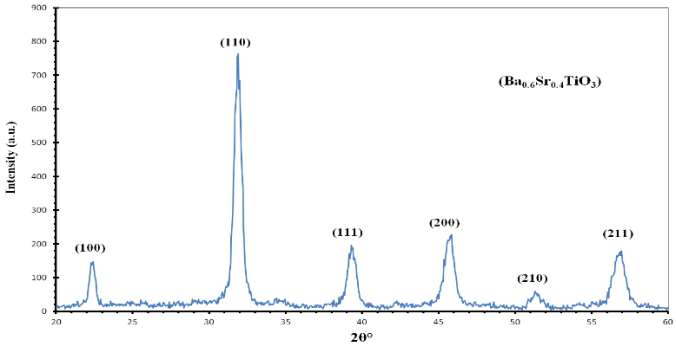

Figure 2. The XRD pattern of BST

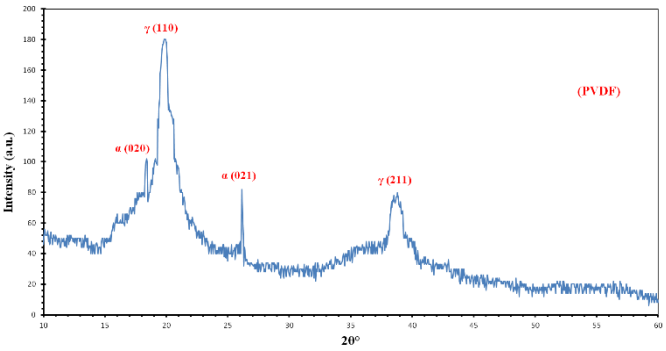

Figure 3. The XRD pattern of PVDF

Figure 4 shows XRD patterns of the PVDF/BST nanocomposites. The strong diffraction peaks of γ - PVDF appearing at 2θ = 19.1° (002), 20° (110) and 26.9° (022), and the peaks at 2θ = 17.6° (100), 18.4° (020), were related to α-PVDF [14]. The peaks at 2θ = 22°, 31°, 39°, 45° and 56° referred to (100), (110), (111), (200), and (211) planes of BST.

From the X-ray data for PVDF/BST nanocomposites, it can be observed that the strongest peak occurs at 2θ=20° which is referred to (110) plane of γ – PVDF. The intensities of diffraction peaks of γ – PVDF and α – PVDF were decreased and the peaks at 2θ =17.6° (100), 18.4° (020), 26.9° (022),

were disappeared with the increasing of content of BST filler but the contrary happened to the diffraction peaks of BST.

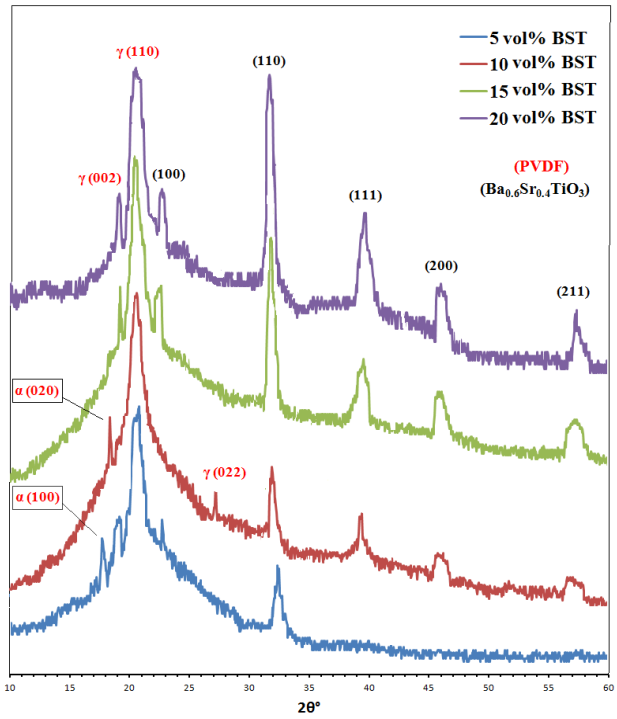

Figure 4. The XRD patterns of the PVDF/BST composites with different filler contents

The average crystallite size for the samples is calculated by using Scherrer's equation [15]:

$$D = k\lambda/\beta\cos\theta \quad \ldots\ldots\ldots(1)$$

where D is the average crystallite size λ is the x-ray wavelength of CuK_α (λ = 1.54178 A), β is full width at half maximum (FWHM), θ is Bragg's angle, and k=0.9.

The average crystallite size for the samples can be determined using Williamson-Hall (W-H) equation shown below [15]:

$$\beta\cos\theta = \frac{k\lambda}{D} + 4S\sin\theta \quad \ldots\ldots\ldots(2)$$

where S is the microstrain in the sample. If βcosθ is plotted with respect to 4sinθ for all peaks, microstrain and crystallite size can be calculated from the slope and y-intercept of the fitted line respectively as shown in Figure 5. Table 1 show microstrain and average crystallite size for the samples calculated by Scherrer and Williamson-Hall (W-H) equations. It is observed that the crystallite size increase as the content of BST filler increases from 5 to 20 vol%. These results agree qualitatively with the results of crystallite size obtained by Williamson-Hall method. The observed increase in microstrain is due to slight deformation in crystalline structure, and the negative value indicates the occurrence of compression in the lattice [16].

Table 1: Average crystallite size and microstrain of PVDF/BST composites with different filler contents

Sample	D nm (Scherrer)	D nm (W-H)	microstrain %
5 vol% BST	9.03	9.06	0.17
10 vol% BST	9.25	11.75	0.37
15 vol% BST	9.05	9.49	0.12
20 vol% BST	9.59	9.83	-0.02

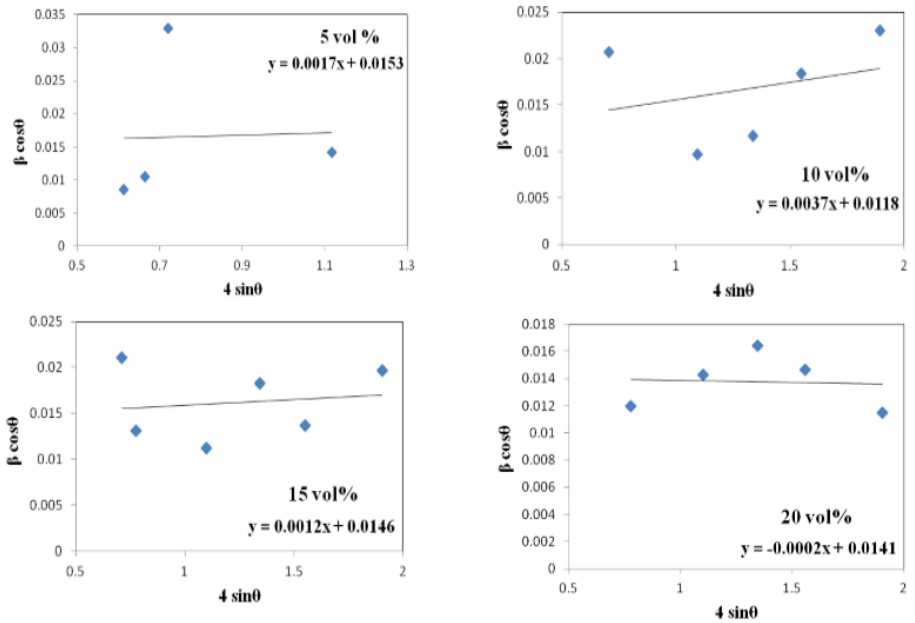

Figure 5. Williamson-Hall analysis of the PVDF/BST composites with different filler contents

Figure 6 and Figure 7 show the frequency dependency of dielectric constant and dielectric losses of the PVDF/BST naocomposites with different volume fractions of BST filler in frequency range 50Hz–1MHz at room temperature. In Figure 6, one can see that the dielectric constant for the composite 20 vol% BST has the highest dielectric constant value and PVDF film are the lowest. This confirms that the dielectric constant increases with the increasing of volume fraction of BST filler at the same frequency, which should be attributed to the considerably higher dielectric constant of BST in comparison with that of the PVDF. The dielectric constant of all the composites decreases with the increasing of frequency. The phenomenon can be attributed to the polarization relaxation occurring at the inner structure of composites, including interface polarization and dipole orientation polarization.

The dielectric losses of PVDF/BST composites measured in the frequency range from 50Hz to 1MHz at room temperature is shown in Figure 7. The dielectric losses increase slowly with the increasing of volume fraction of BST filler at the same frequency, and the dielectric losses of all the composites decreases with the increasing of frequency.

The A.C conductivity of PVDF/BST composites was calculated from the relation [17]:

$$\sigma_{ac} = 2\pi .f. \varepsilon_0 . \varepsilon'' \quad \text{.....(3)}$$

Where σ_{ac} is the AC conductivity, f is the applied frequency, ε_o is the permitivity of free space, and ε'' is the dielectric losses of the samples.

Figure 8 shows the AC conductivity of PVDF / BST composites measured in the frequency range from 50Hz to 1MHz at room temperature. It can be observed from the figure that the AC conductivity increase with the increasing of volume fraction of BST filler at the same frequency, and showed a continuous increasing with the increasing of the applied frequency for all the composites.

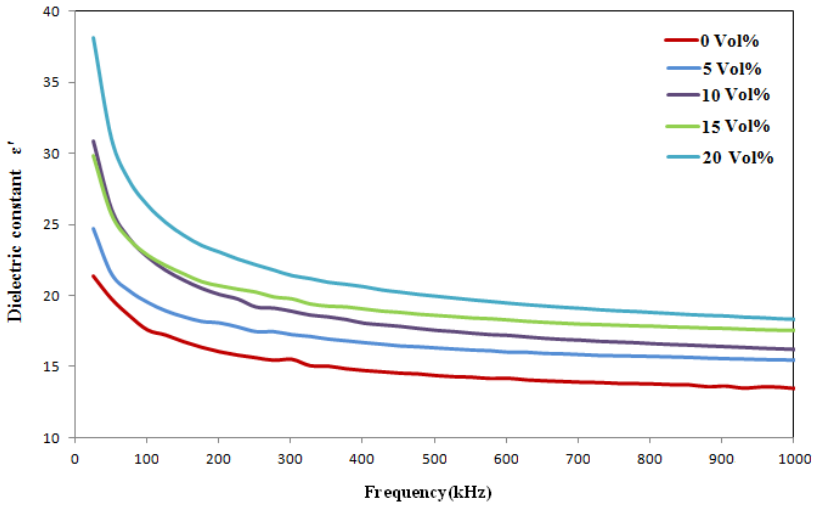

Figure 6. Dielectric constant as a function of frequency of the PVDF/ BST composites with different filler contents.

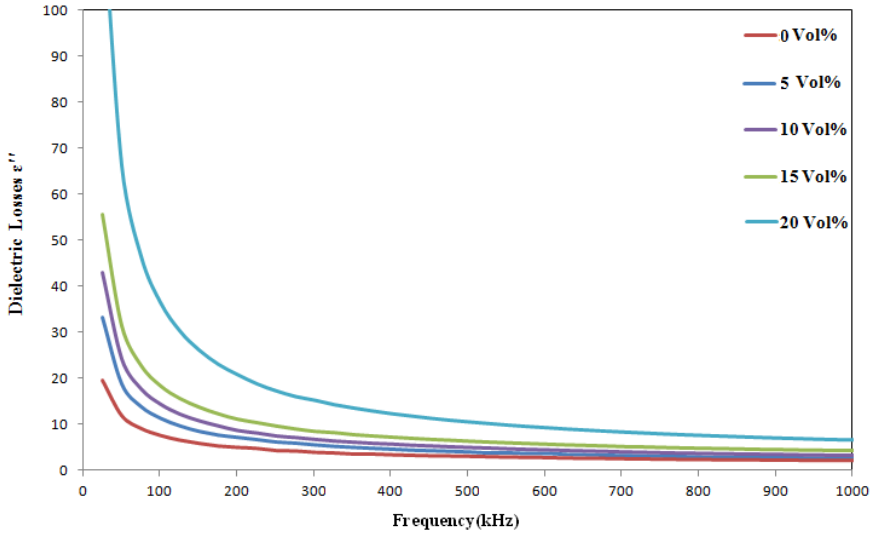

Figure 7. Dielectric losses as a function of frequency of the PVDF/BST composites with different filler contents.

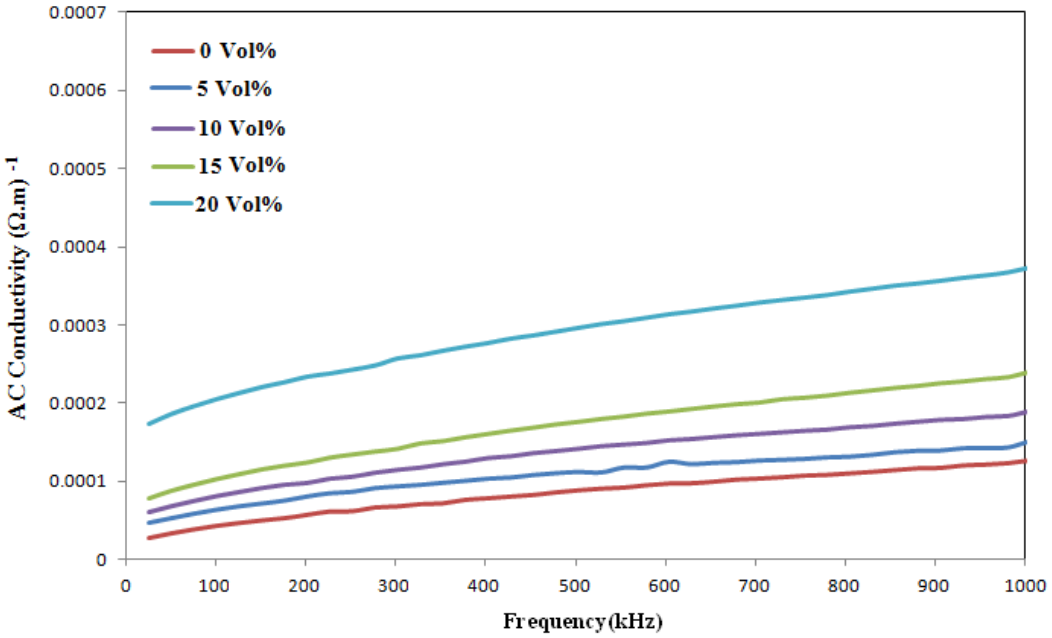

Figure 8. AC Conductivity as a function of frequency of the PVDF/BST composites with different filler contents.

CONCLUSIONS

In this study PVDF/BST nanocomposites with different filler content were fabricated by using solution casting method. The XRD results showed the perovskite structure of BST nanoparticals and the α and γ - PVDF crystalline phases appeared at pure PVDF and nanocomposites samples. The crystallite size increase as the content of BST filler increases from 5 to 20 vol.%. The dielectric constant, dielectric losses and AC conductivity of the PVDF/BST nanocomposites increase with BST filler increasing at the same frequency. AC conductivity showed a continuous increasing with the frequency increasing for all the composites.

REFERENCES

[1] Lovinger, A.J., 1983, "Ferroelectric polymers," Science, 220(4602), pp.1115-1121.

[2] Nalwa, H.S., 1995, "Ferroelectric polymers: chemistry: physics, and applications, " CRC Press.

[3] Yu, K., Wang, H., Zhou, Y., Bai, Y. and Niu, Y., 2013, "Enhanced dielectric properties of $BaTiO_3$/poly (vinylidene fluoride) nanocomposites for energy storage applications," Journal of applied physics, 113(3), p.034105.

[4] Dang, Z.M., Yu, Y.F., Xu, H.P. and Bai, J., 2008, "Study on microstructure and dielectric property of the $BaTiO_3$/epoxy resin composites," Composites Science and Technology, 68(1), pp.171-177.

[5] Adikary, S.U., Chan, H.L.W., Choy, C.L., Sundaravel, B. and Wilson, I.H., 2002, "Characterisation of proton irradiated $Ba_{0.65}Sr_{0.35}TiO_3$/P (VDF-TrFE) ceramic–polymer composites," Composites science and technology, 62(16), pp.2161-2167.

[6] Bai, Y., Cheng, Z.Y., Bharti, V., Xu, H.S. and Zhang, Q.M., 2000, "High-dielectric-constant ceramic-powder polymer composites," Applied Physics Letters, 76(25), pp.3804-3806.

[7] Alexandru, H.V., Berbecaru, C., Stanculescu, F., Ioachim, A., Banciu, M.G., Toacsen, M.I., Nedelcu, L., Ghetu, D. and Stoica, G., 2005, "Ferroelectric solid solutions (Ba, Sr) TiO3 for microwave applications, " Materials Science and Engineering: B, 118(1-3), pp.92-96.

[8] Sencadas, V., Moreira, M.V., Lanceros-Méndez, S., Pouzada, A.S. and Gregório Filho, R., 2006, "α-to β Transformation on PVDF films obtained by uniaxial stretch," Materials science forum, 514, pp. 872-876).

[9] Kepler, R.G. and Anderson, R.A., 1978, "Piezoelectricity and pyroelectricity in polyvinylidene fluoride," Journal of Applied Physics, 49(8), pp.4490-4494.

[10] Chiang, C.K. and Popielarz, R., 2002, "Polymer composites with high dielectric constant," Ferroelectrics, 275(1), pp.1-9.

[11] Ishida, H., Campbell, S. and Blackwell, J., 2000, "General approach to nanocomposite preparation," Chemistry of Materials, 12(5), pp.1260-1267.

[12] Liu, S. and Zhai, J., 2014, "A small loading of surface-modified $Ba_{0.6}Sr_{0.4}TiO_3$ nanofiber-filled nanocomposites with enhanced dielectric constant and energy density," RSC Advances, 4(77), pp.40973-40979.

[13] Attar, A.S., Sichani, E.S. and Sharafi, S., 2017, "Structural and dielectric properties of Bi-doped barium strontium titanate nanopowders synthesized by sol–gel method," Journal of materials research and technology, 6(2), pp.108-115.

[14] Martins, P., Lopes, A.C. and Lanceros-Mendez, S., 2014, "Electroactive phases of poly (vinylidene fluoride): determination, processing and applications, " Progress in polymer science, 39(4), pp.683-706.

[15] Mote, V.D., Purushotham, Y. and Dole, B.N., 2012, "Williamson-Hall analysis in estimation of lattice strain in nanometer-sized ZnO particles," Journal of Theoretical and Applied Physics, 6(1), p.6.

[16] Medhi, N. and Nath, A.K., 2013, "Gamma ray irradiation effects on the ferroelectric and piezoelectric properties of barium titanate ceramics," Journal of materials engineering and performance, 22(9), pp.2716-2722.

[17] Roy, A.K., Singh, A., Kumari, K., Prasad, K. and Prasad, A., 2013, "Electrical conduction in $(Bi_{0.5}Na_{0.5})_{0.94}Ba_{0.06}TiO_3$-PVDF 0-3 composites by impedance spectroscopy," Journal of Applied Physics, 3(5), pp.47-58.